Computational and Structural Biotechnology Journal 17 (2019) 215–228

COMPUTATIONAL AND STRUCTURAL BIOTECHNOLOGY JOURNAL

journal homepage: www.elsevier.com/locate/csbj

Effects of Lid 1 Mutagenesis on Lid Displacement, Catalytic Performances and Thermostability of Cold-active Pseudomonas AMS8 Lipase in Toluene

Norhayati Yaacob [a,b], Nor Hafizah Ahmad Kamarudin [b], Adam Thean Chor Leow [b,c], Abu Bakar Salleh [b], Raja Noor Zaliha Raja Abd Rahman [b,d], Mohd Shukuri Mohamad Ali [b,e,*]

[a] Enzyme Technology Laboratory, Laboratory of Molecular Biomedicine (MOLEMED), Institute of Bioscience, Universiti Putra Malaysia, 43400 Serdang, Malaysia
[b] Enzyme and Microbial Technology Research Centre, Faculty of Biotechnology and Biomolecular Sciences, University Putra Malaysia, 43400 Serdang, Malaysia
[c] Department of Cell and Molecular Biology, Faculty of Biotechnology and Biomolecular Sciences, Universiti Putra Malaysia, 43400 Serdang, Malaysia
[d] Department of Microbiology, Faculty of Biotechnology and Biomolecular Sciences, Universiti Putra Malaysia, 43400 Serdang, Malaysia
[e] Department of Biochemistry, Faculty of Biotechnology and Biomolecular Sciences, Universiti Putra Malaysia, 43400 Serdang, Malaysia

ARTICLE INFO

Article history:
Received 7 November 2018
Received in revised form 14 January 2019
Accepted 19 January 2019
Available online 25 January 2019

Keywords:
Lid engineering
Cold-active lipase
Molecular dynamics simulation
Hydrophobic contacts
Site-directed mutagenesis
Solvent accessibility
Substrate affinity
Thermostability

ABSTRACT

Pseudomonas fluorescens AMS8 lipase lid 1 structure is rigid and holds unclear roles due to the absence of solvent-interactions. Lid 1 region was stabilized by 17 hydrogen bond linkages and displayed lower mean hydrophobicity (0.596) compared to MIS38 lipase. Mutating lid 1 residues, Thr-52 and Gly-55 to aromatic hydrophobic-polar tyrosine would churned more side-chain interactions between lid 1 and water or toluene. This study revealed that T52Y leads G55Y and its recombinant towards achieving higher solvent-accessible surface area and longer half-life at 25 to 37 °C in 0.5% (v/v) toluene. T52Y also exhibited better substrate affinity with long-chain carbon substrate in aqueous media. The affinity for pNP palmitate, laurate and caprylate increased in 0.5% (v/v) toluene in recombinant AMS8, but the affinity in similar substrates was substantially declined in lid 1 mutated lipases. Regarding enzyme efficiency, the recombinant AMS8 lipase displayed highest value of k_{cat}/K_m in 0.5% (v/v) toluene, mainly with *p*NPC. In both hydrolysis reactions with 0% and 0.5% (v/v) toluene, the enzyme efficiency of G55Y was found higher than T52Y for *p*NPL and *p*NPP. At 0.5% (v/v) toluene, both mutants showed reductions in activation energy and enthalpy values as temperature increased from 25 to 35 °C, displaying better catalytic functions. Only T52Y exhibited increase in entropy values at 0.5% (v/v) toluene indicating structure stability. As a conclusion, Thr-52 and Gly-55 are important residues for lid 1 stability as their existence helps to retain the geometrical structure of alpha-helix and connecting hinge.

1. Introduction

The structure-guided protein engineering is a strategy used to identify and regulate the molecular interactions happening around certain area of interest which involved in enzymatic functions so that it can be develop into a compelling biocatalyst for industrial applications [1]. Amid many industrial enzymes, lipases contribute to many important roles in biocatalysis process due to its extensive usages in detergents formulation, food preservations and flavorings, biodiesel productions and cosmetics active ingredients [2]. In some lipases, a mobile amphipathic structure known as lid mainly covers the catalytic active site region where the length and complexity of the structure depends entirely on the shape of enzymes. The lid is very much involved in modulating activity and substrate selectivity in lipases. Depending on the target enzymes, protein engineering on lid structures may altered important properties such as enzyme substrate specificity and local stability [3]. In addition, it is often to observe a reduction in enzyme activity whenever lid paves way to selected compounds of increasing lipophilic characteristics. Non-polar solvent such as toluene is one of the medium which supports the solubility of amphipathic molecules/compounds where interactions with lid allowing substrate access to the active site and initiation of catalysis. The intrinsic conformational changes of the enzyme initiated by lid domain are important determinants for lipase activation especially in organic solvents [4].

Mutations on lid sequence would cause in different interactions of enzyme towards the presence of organic solvents. Previously, the lid engineered *Candida rugosa* lipase activity and enantioselectivity was found reduced in organic solvents. Cold-active *Pseudomonas fragi* lipase has its chain length specificity altered while experiencing an increase in

* Corresponding author.
E-mail address: mshukuri@upm.edu.my (M.S.M. Ali).

https://doi.org/10.1016/j.csbj.2019.01.005

thermostability, also in the presence of organic solvents [5]. Later, Jørgensen et al. described that lipase would undergo structural transition from close to open state when being exposed to high solvent polarities [4]. Normally, lid has a weaker tendency to orient itself in a preferred orientation between a polar and apolar medium. In the case of *Thermomyces lanuginosus* lipase E87K, a negatively-charged residues such as glutamic acid (E) that serves to stabilize the lid in a closed conformation can potentially be mutated with an opposite charge residue such as lysine (K) to allow lipase activation at high solvent polarities. This amino acid substitution on α-helix domain results in increase of energy needed to activate lid opening at low dielectric constants [4]. As the enzyme shifts to the open conformation, the hydrophobic interphase was exposed, making the enzyme even more accessible to substrate. In the meantime, lid replacement in *Candida rugosa* lipase has resulted in substrate-independent hydrolysis reaction of p-nitrophenolesters which responded to added detergents. The change in lid position by detergent was stimulated by the shift of reaction equilibrium of different conformation state in detergent/interfaces [6]. In cold adapted enzymes, the lid modulation depends on the conformational flexibility as part of a molecular adaptation towards consistency of interactions between lid and its surroundings [7]. Thus, it is frequently said that lid appears to display a very complex role in lipases activity, specificity and conformational stability subjected to variations of amino acid sequences and its surrounding. In addition, surface accessibility is important for any residue involved with exterior interactions [8].

Previous works highlighted the importance of the lid sequence to structure, mechanism and function via protein engineering (lid swapping and site-directed mutagenesis) and computational analysis focusing on lid domain. Based on these approaches, the role of the lipase lid in substrate selectivity and activity in the presence of solvents or surfactants or detergents can be identified. In lipases, lid was observed to have a distinct appearance in three groups. The first ones are lipases without lid, secondly, lipases with one loop or one helix lid and the last ones are lipases with two or more helical lids [9]. Cold-active *Pseudomonas fluorescens* AMS8 lipase shared similarity to lid sequence from lipase of *Pseudomonas* sp. MIS38, and thermophilic lipases from *Proteus mirabilis* and *Geobacillus stearothermophilus* [10,11,12], where these lipases clearly showed to have two helical lids [8]. Lid 1 is a short-hingedalpha-helix lid located at residue 51–57 and is found inactive (structurally rigid) in the presence of organic solvent, whereas the second and longer alpha-helix lid 2 (148-167) is saturatedly composed with hydrophobic residues. Unlike lid 1, the role of lid 2 in interfacial activation and substrate accessibility has been associated with interactions in non-polar organic solvents.

The main objective of this work is to determine the effects of lid 1 mutation to physical and biochemical properties of cold-active *Pseudomonas* AMS8 lipase in hydrophobic/aqueous interphase. It is hypothesized that higher activity of lipase could be achieved in toluene if lid 1 gets shifted from 'close' to 'open' state conformation via increased in solvent-surface interactions. By making lid 1 to co-participate lid 2 in the activation of lipase, the barriers in obtaining higher lipase activity could be overcome. In current state, it was difficult to understand the catalytic behavior of cold-active lipase with two lids where the function relies heavily on lid activation and its biomechanics. In the context of current study, lid activation involves the voluntary opening and closure of alpha-helix structure in organic solvent via surface interactions to stimulate better catalysis.

2. Materials and Methods

2.1. Prediction of Protein Stability, Solvent-accessibility and Flexibility of Lid 1 Mutant Candidates

The knowledge-based approach was used to predict the effects of site-directed mutagenesis (SDM) on protein stability and to calculate the change in thermal stability between recombinant and mutant lipases (http://marid.bioc.cam.ac.uk/sdm2/). PDB file containing the 3D coordinates of the protein atoms of AMS8 lipase was submitted to the server. Following this, a summary of analysis is presented, stressing on details of the recombinant and mutant residues, residue number and protein chain. Another list features the prediction analysis of mainchain conformation, side-chain solvent accessibility, side-chain hydrogen bonding pattern for both recombinant and mutant residues [13]. The physico-chemical features of α-helix sequence of lid 1 (51–57) and its outskirt (+ 5) residues in recombinant AMS8 lipase was explored via online server, HeliQuest (http://heliquest.ipmc.cnrs.fr/cgi-bin/ComputParams.py). This module allows specific properties such as hydrophobicity, hydrophobic moment, net charge (z) and amino acid composition for several helix types to be determined.

2.2. Lid 1 Mutant Designed, Expression, and Purification

A polar Thr-52 and neutral Gly-55 located at the center of lid 1 region were chosen as the target for mutation and substituted with tyrosine which has aromatic side chain and hydroxyl group at its benzene ring making it semihydrophobic. Mutant T52Y and G55Y lipases were obtained by site-directed mutagenesis using a previous construct recombinant pET32b-AMS8 plasmid as DNA template [14,15]. Primers used for rational mutagenesis were designed via web-based automated program, QuikChange Primer Design (http://www.genomics.agilent.com/primerDesignProgram.jsp) and synthesized by Life Technology (Guangzhou, China) as shown in Table 1.

A recombinant lipase with expression vector pET32b + harboring mutation site was prepared by using QuikChange Lightning Site-Directed Mutagenesis kit (Catalog No. #210519, Agilent Technologies, USA) where a few colonies were sterilely picked and plasmid extracted for sequencing. The positive lid 1 mutant lipases were then digested with restriction enzymes, BamH1 and *Xho*I (NEB, USA) and re-transformed into expression host, *E. coli* BL21 (DE3) from Novagen®, Germany.

Subsequent expression and purification of recombinant AMS8 and its mutant lipases were carried out according to the methods previously described [15]. In brief, both recombinant AMS8 and lid 1 mutant lipases (T52Y and G55Y) were expressed as fusion protein with histidine binding domain tag for the purpose of affinity purification via Nickel-Sepharose Excel (GE, USA) followed by anion-exchange chromatography (IEC) purification by using 2 × 5 mL pre-packed column of HiTrap Q HP (GE, USA). The purified proteins were collected, pooled and concentrated by ultra-centrifugation (Amicon, Merck). The purity of expressed lipase was analysed by sodium dodecyl sulfate polyacrylamide gel electrophoresis (SDS–PAGE) [16]. Protein concentrations were measured by using Bio-Rad Protein Assay (Bio-Rad Laboratories, USA) [17].

2.3. Molecular Dynamics (MD) Simulations of Recombinant and Mutated Lid 1 AMS8 Lipase

The MD simulations were performed on computed model of recombinant AMS8 and lid 1 mutant lipases using YASARA structure software (version 11.3.22, Netherlands) following previous MD settings and protocols in water or toluene [7,18] targeting specific temperature of 25 °C and 37 °C. The system was equilibrated at the steepest descent parameters, using a time step of 1 fs for intramolecular forces which calculated the intermolecular forces in every 2 simulation sub-steps. The structure was energy-minimized with AMBER03 force field using a cut off 10.486 Å and the Particle Mesh Ewald algorithm to treat long range electrostatic interactions. After the removal of conformational stress by a short steepest descent minimization via 50 steps of MD in solvent, the procedures continued by simulated annealing and converge as soon as the energy improves by <0.05 kJ/mol per atom within 200 steps. The changes of protein structure were examined using 800 saved

Table 1
Primer sequences designed for site-directed mutagenesis.

Area of mutation	Mutation site	Forward sequence (5′–3′)	Reverse sequence (5′–3′)	Annealing temperature (°C)
Lid 1	T52Y	GGCTGCCGGCATATCTGGTGGGGG	GCCCCCACCAGATATGCCGGCAGCC	69
	G55Y	CAACCCTGGTGTATGCGCTGCTTGG	CCAAGCAGCGCATACACCAGGGTTG	64

trajectories where each 40 simulation snapshots represents 1 ns. The MD simulation was allowed to run until 20 ns. By using final trajectories from MD simulations, the hydrogen-bond networks in recombinant AMS8 and mutant lipases, T52Y and G55Y were explored by BIOVIA Discovery Studio 2017R2 Visualiser version 17.2.0.16,349 (Dassault Systemes, 2016).

2.4. Normal Mode Analysis (NMA) and Sequence-specific Solvent Accessibilities (ProtSA) Analysis of Lid 1 Mutants

Normal mode analysis (NMA) is a fast and simple method to calculate vibrational modes and protein flexibility [19]. To get this information, the final trajectories of simulated lipase in toluene was taken and submitted to Elastic Network Model (ENM) website: http://www.sciences.univ-nantes.fr/elnemo/. ENM is an algorithm that enables quantitative description of protein behaviour starting from three dimensions (3D) view of protein assemblies to the network models showing the connecting pairs of nodes located within a distance measured under harmonic restrictions from the equilibrium structure [19]. The application offers calculations of normal or vibrational modes on all atoms by fixing it on Cα.

ProtSA calculates sequence specific protein solvent accessibilities in the unfolded ensemble by simulating the unfolded protein many times and combining the results. In the simulations, the structural model to describe the unfolded conformations representative of the unfolded protein is generated by the Flexible-Meccano algorithm [20]. The analytical software ALPHASURF is applied to calculate atom solvent accessibilities. The tool was readily available for download at: http://webapps.bifi.es/protsa/#Xbernado:2006.

2.5. Biochemical Properties of AMS8 Lipase and its Mutant

The hydrolysis activity of AMS8 and lid 1 mutant lipases was measured spectrophotometrically by using Kwon and Rhee method [21]. The enzyme kinetics was measured by *p*-nitrophenyl caprylate (pNP-C8), laurate (pNP-C12) and palmitate (pNP-C16) as substrates. Each reaction mixture consists an approximate 10 μl purified lipase (AMS8, T52Y and G55Y) with 100 μg total protein concentration, 175 μl of buffer 50 mM Tris-HCl, 4% (v/v) 2-propanol and 1% (v/v) acetonitrile (all mixed to pH 8), 5 μl of 50 mM $CaCl_2$ and 10 μl of toluene. Together with enzyme, the assay mixture was equilibrated for 5 min at 25 °C (fixed temperature kinetic) or 25–45 °C (for Arrhenius plot) in the multiplate reader (BioTek Synergy, USA). Just before reaction, about 10 μl of 20 mM pNP solution dissolved in 2-propanol was spiked into each well. Both negative (excluding enzyme) and positive (excluding substrate) assay control were performed in every measurement as part of a blank. The reaction time was 3 min, and the absorbance was read in every 12 s at 405 nm [22]. One unit of enzyme activity is defined as the rate of release of 1 μmole pNP per minute under assay conditions. Substrate specificity (K_m) and k_{cat} were determined either by Haneswoolf (half-reciprocal) plot of [S]/v against [S] or Lineweaver-burk plot of (1/V) against 1/[S] and compared.

2.6. Secondary Structure, Melting Temperature (T_m) and Aggregation Point (T_{agg}) Analysis

The solvent effect on secondary structures of recombinant AMS8 and lid 1 mutant lipases was determined from 190 to 280 nm by using Circular Dichroism (CD) spectropolarimeter (model J-810, JASCO, Japan) at 20 °C, 25 °C and 30 °C using 0.5 mg/ml of purified protein in 10 mM Tris-HCl, 5 mM $CaCl_2$ buffer (pH 8.0). CD scanning was performed and analysed with averaged data from three replicates. Secondary structure results were analysed by using Raussens et al., 2003 method [23].

Melting temperature (T_m) of all lipases was measured with CD at 222 nm and temperature range 20–70 °C. T_m can be defined as temperature that denatures 50% of incubated protein. Sample contained purified protein at 0.4 mg/ml was prepared in buffer 20 mM Tris-HCl, 5 mM $CaCl_2$ pH 8 as a baseline to enable data collection. Since the mixture of protein and toluene creates an undesired non-homogenous solution, the recommended limit of organic solvent concentration used for T_m analysis by in-house CD was up to 5% (v/v). The path length of cell cuvette used was 0.2 cm and the internal temperature of CD was set at 20 °C.

The formations of protein aggregation in purified mutant lipases were determined in the presence of 0.5% (v/v) toluene. Protein sample (~0.3–0.5 mg/ml) prepared in 50 mM Tris–HCl, 5 mM $CaCl_2$ buffer (pH 8.0) was used for Dynamic Light Scatterings (DLS) measurement from 20 to 70 °C. Data were analysed using Zetasizer software (v 7.11) to compare reduction in molecular size (d.nm) or volume size of proteins after experienced increase of temperature with and without toluene (0.5%, v/v).

2.7. Thermodynamic Analysis

Both recombinant AMS8 and mutant lipases were purified and assayed in substrate, *p*NPC at different temperatures (25–45 °C) for the determination of k_{cat} and to plot Arrhenius graph. Activation energy (Ea) of respective lipases was calculated by identifying the slope of Arrhenius graph showing a series of data in ln k_{cat} against 1/T (K^{-1}). or, alternatively by calculating Ea by means of formula:

$$\ln\left[\frac{k_2}{k_1}\right] = \frac{-Ea}{R}\left[\frac{1}{T_2} - \frac{1}{T_1}\right] \quad (1)$$

where, T_1 and T_2 is the temperature in Kelvin (K) at 25 °C and 35 °C. k_1 and k_2 is the k_{cat} of lipase activity in *p*NPC measured at 25 °C and 35 °C, respectively.

As for measuring Gibbs-free activation energy (ΔG‡), enthalpy (ΔH‡), and entropy (ΔS‡) per single temperature, equations were used for calculation [24,25]. The magnitude of energy required to achieve the same position of equilibrium in both forward and reverse reactions can be explained in terms of various thermodynamic parameters such as changes of Gibbs free energy (G), enthalpy (H) and entropy (S) for both reactants and products involved in a reaction [26].

$$\Delta G‡ = RTx\left[\ln\left[\frac{k_B T}{h}\right] - \ln k\right] \quad (2)$$

$$\Delta H‡ = Ea - RT \quad (3)$$

$$\Delta S‡ = (\Delta H‡ - \Delta G‡)/T \quad (4)$$

In the above equations, k_B is the Boltzmann constant (1.3805 × 10–23 J·K^{-1}), *h* is the Plank constant (6.6256 × 10^{-34} J.s), *k* is the catalytic rate constant, and R is the gas constant (8.314 J mol^{-1} K^{-1}) [24].

3. Results and Discussion

3.1. Preliminary Analysis and Outcome Predictions on Lid 1 Mutation

Lipases with special properties such as thermostable, organic solvent friendly and active at broad temperatures receive great industrial attention because of their usability under restricted reaction condition [27]. In this study, AMS8 lipase was special due to its ability to tolerate the harshness of organic solvent. Cold-active AMS8 lipase behaved as a soluble protein in water and so did other polar organic solvents. Even though the lipase is soluble, polar organic solvents had shown to cause in the destabilization of the protein structure. In addition, polar organic solvent was found not to stimulate lid activation like non-polar organic solvent did [18]. This was because the structure flexibility exhibited by lid 2 regions (148–167) enabled the lid to open and formed a tunnel for the substrate to move into the catalytic pocket. Hydrophobic core was exposed after lid was flipped to the side which attracting the non-soluble and lipid-based substrate to bind. The contributions between AMS8 lid structure and non-polar solvent interactions improves protein surface interactions as it enhances lipase catalysis in organic solvent especially toluene. AMS8 lipase possessed two lids and with molecular simulation, only lid 2 showed an observable movement upon non-polar solvent contact which was not detected at lid 1 (51–57). In MIS38 *Pseudomonas lipase*, there are two lids (lid 1: residues 140–167 and lid 2: residues 46–74) that harbour similarity in sequence homology to the currently studied AMS8 lipase. In this context, the lids in AMS8 lipase were each addressed as lid 1 for residues 51–57 and lid 2 for residues 148–167, opposite to MIS38 naming of lid. In *Pseudomonas* MIS38 lipase, both lids exhibited movement and sustain open conformation in aqueous environment [28]. The role of hydrophobic interactions in MIS38 lipase interfacial activation has been confirmed by the presence of proline which acts as a hinge residue to its lid 2 helix situated at residue 50. Meanwhile in *Aspergillus niger* lipase, prolines in the hinge domain of lid serve to stabilize the open lid conformation as a mean of substrate entry [4]. The lid 2 sequence in MIS38 lipase was "PATLVTALLGG". In this study, AMS8 lipase lid 1 sequence was differentiated by two residues, Gly-55 and Ser-60 – "PATLVGALLGS". These two amino acids substitutions would have caused lid 1 to adopt a rigid structure instead of a flexible one. In AMS8 lipase, Gly-55 has a lighter residue weight compared to Thr-55 but Ser-60 might help in establishing an intramolecular H-bonding with Gly-55 making the region highly stable and movement restricted. Ser-60 also was found to be the reason behind the lack of hydrophobic interface of lid 1 as shown in Table 2.

The movement of an α-helical lid by rotating around two hinge regions at the lipid-water interface created a hydrophobic patch surrounds the catalytic triad, resulting in activation of the lipase [29]. Instead of changing the residues of alpha-hinge Ser-60 to Gly-60 to make available on hydrophobic patch, this study focused on to improve the flexibility of the lid domain (in this case lid 1) by providing anchor (via side-chain interactions) to toluene on the alpha-helix surface of lid 1 as alternative approach for "interfacial activation" and to enforce the mobility of these H-bond saturated area by allowing the hinge to move about freely.

Our interest is to improve the hydrophobic interactions for better surface activation in non-polar organic solvent at lid 1 (51–57) by targeting residues Thr-52 and Gly-55. At pH 8, both Thr-52 and Gly-55 were found to be uncharged and to promote interactions with non-polar organic solvent, aromatic residues such as Tyr, Trp and Phe could offer better hydrophobic interactions. However, assigning an aromatic residue to a small alpha-helix lid could alter the coordination of lid in facing active site. A close check on peptide sequences showed that lid 1 was built by a successive arrangement of polar, neutral (no charge) and hydrophobic-aliphatic amino acids which do not attract any bond formations or ionic interactions between their side chains

Table 2
Helical domain analysis (46–63) in MIS38, AMS8 and lid 1 mutant lipases. This analysis showing the distribution of amino acid residues and the orientation of the amphipathic moments (black arrows) calculated on the basis of the hydrophobicity and side chain distribution of the amino acids in the helices.

Name of lipase	Alpha-helix domain 46-63	Mean hydrophobicity	Hydrophobic moment	Hydrophobic patch (residues)	Helical wheel of alpha-helix domain 46-63	Close-up view of lid 1 and hinge	Total no. of hydrogen bonds (residues 49-59)
MIS38 lipase (2Z8Z) -reference	**GLGLPAT LVTALLG GTDS**	0.613	0.276	A_{56} L_{49} G_{60} L_{53} G_{46} L_{57} P_{50}	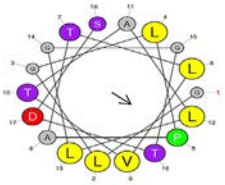		13
Recombinant AMS8	**GLGLPAT LVGALLG STDS**	0.596	0.287	A_{56} L_{49} S_{60} L_{53} G_{46} L_{57} P_{50} (none)	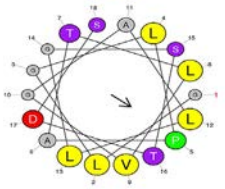	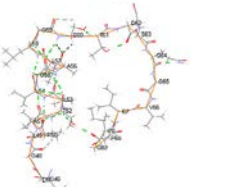	**17**
T52Y	**GLGLPAY LVGALLG STDS**	0.635	0.252	A_{56} L_{49} S_{60} L_{53} G_{46} L_{57} P_{50} (none)	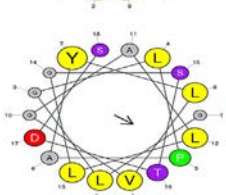	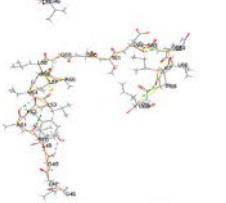	10
G55Y	**GLGLPAT LVYALLGS TDS**	0.649	0.246	A_{56} L_{49} S_{60} L_{53} G_{46} L_{57} P_{50} (none)	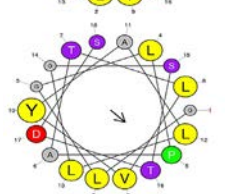	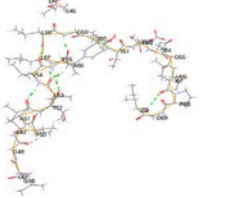	8

and the respective solvents. Site-directed mutagenesis on lid 1 surface could facilitate various approaches associated with function prediction and stability in organic solvent. Based on helix domain analysis highlighting residues 46–63, AMS8 lipase showed a distinct distribution of hydrophobic amino acids in the helix that generates a large amphipathic moment (based on the direction pointed by arrow) supposedly making favourable hydrophobic interactions with the hydrophobic active site (Table 2).

The only difference between AMS8 lipase lid 1 and MIS38 lid 2 helix domain was the availability of hydrophobic patch that display better amphipathic moment. In this case, MIS38 lipase has better hydrophobic interaction with the active site. Both mutations on lid 1 targeting residues Thr-52 and Gly-55 did enhanced the mean hydrophobicity of AMS8 lipase after substitution with Tyrosine. Thr-52 is targeted because it is polar in characteristic and can accommodate rotamers which indicates that side chains adopt unstrained conformation. After being replaced with an aromatic amino acid such as Tyr, differences could be observed between the orientation of side chain and stalking effects with aromatic-organic solvent such as toluene. Although tyrosine is hydrophobic, it has lower pKa due to the presence of phenolic hydroxyl (a polar side group) which makes it ionizable and highly stable on the protein surface. Mutation at Gly-55 (located between hydrophobic-aliphatic Val-54 and Ala-56) was targeted and substituted with Tyr-55 as Gly-55 did not form any important interactions (polar or non-polar) within this region. Both mutation sites especially the side-chain were predicted not to form any H-bond with other neighbouring residues and the differences in free energy strongly indicates that both mutated protein has impact on protein stability and activity as shown in Table 3. The predictions on these potential mutants were assessed through SDM, a useful tool for predicting the effects of a mutation on protein structure and function. In general, computational approaches to predict protein stability (or protein stability changes) is physics-based, knowledge-based, or a hybrid [30].

3.2. Effects of Temperature to Lid 1 Mutation

Temperature-mediated protein interactions has been associated with many changes of enzymatic activities. This makes temperature, one of the crucial factors that trigger lid 2 interfacial activation in cold-active AMS8 lipase other than the hydrophobic organic solvents [7,31]. It would be interesting to see the outcomes of structural changes at the lid area in response to temperature and toluene. Previous simulation of solvent-stable lipase, Lip42 in water-solvent shows the perturbation of hydrophobic clusters and structural changes due to the open-closure of the lid [32]. In this study, the conformational change after lid 1 mutation was not found in 25 °C simulation, except for the large displacement observed in recombinant AMS8 lid 2 residues (Fig. 1 A). However, the change in the conformational movement was found to be linked with lid 1 when both mutants (T52Y and G55Y) were subjected to MD simulation at higher temperature, 37 °C (Fig. 1 B). Recombinant AMS8 lipase appeared to have a low atomic displacement at 37 °C in which both lids turned out rigid and static. Such thermal-inducing motions are central importance to protein function and stability. A slight difference in temperature can influence the flexibility of cold-active lipase via disruption on its interfacial lid. At first, lid 1 did not assume to its role in lid activation under its normal temperature, 25 °C but after mutation, a significant difference could be observed at 37 °C in the presence of toluene.

Based on molecular dynamics analysis, lid 1 and lid 2 undergoes conformational changes with increase of temperature. Most importantly, lid 1 appeared to respond towards moderate temperature, 37 °C probably requiring higher force to stimuli its recognition to the presence of toluene. By raising the temperature to 37 °C, Gly-69 exhibited greater flexibility in T52Y and AMS8 recombinant lipase (Fig. 2A,Fig. 2 B). The reason behind it is that, Gly-69 could not interact strongly with other neighbouring residues that are hydrophobic. Therefore, direct exposure of this residue to the non-polar solvents might trigger the flexibility. In terms of property, Glycine has no side chain and electrostatic charges which make the residue easily moved by surface bound water molecules via hydrophilic interactions. This highly flexible Gly-69 could also be the starting point of protein unfolding due to their large fluctuation and disorientations. The catalytic effects caused by Gly-69 flexibility can be observed through a slight increase of catalytic rate (k_{cat}) at 35 °C. However, the activation energy required for lipase activity to occur is found higher in toluene at 25–35 °C probably due to the restricted flexibility of lid 2 when temperature starts to increase. At 37 °C, lid 2 responded by showing reductions in RMSf value. A declined lid 2 flexibility of recombinant AMS8 lipase means that overall structure of lipase became highly stable at 37 °C and required more activation energy for lipase activity.

As for T52Y, lid 1 and lid 2 were greatly affected by temperature increase (Fig. 2 B). The high RMSf value of Gly-69 at 37 °C showed that T52Y capable of changing the structure of lid 1 and lid 2, while a lower RMSf values in G55Y indicated that this mutation had brought no effect towards change of lid 1 structure in particular of that site (Fig. 2 C). Interestingly, Gly-69 was found located at the posterior hinge domain of lid 1 that could have influenced the subsequent shift (in RMSf) of lid 1 at 37 °C. In this study, simulation induced by temperature showed a significantly large fluctuating area on lid 1 aided by the presence of toluene. Lid 1 might have special roles and it could be based on mutual dynamics of both thermostability and solvent-recognition. Previously, activity measurements and MD simulations on psychrophilic AMS8, M37 and thermophilic *Thermomyces lanuginosus* lipase (TlL) suggest that the opening of the lid is energetically unfavorable in aqueous solutions until temperature or hydrophobic solvent triggered the interface activation [15,33,34].

Fig. 3 (A) shows that by changing the temperature from 25 °C to 37 °C, the RMSd values of recombinant lipase AMS8 declined from 7 Å to 4 Å. The reductions of RMSd values in mutant T52Y were also reported following increased in temperature. At 25 °C, T52Y showed a sharp irregular increase of RMSd between 0 and 5 ns before slowly declined to 5 Å and stabilized at 4 Å until the simulation reached 20 ns. In contrast, G55Y showed no difference in terms of overall RMSd values at both temperatures showing no significant changes on average distance, stressing on close similarity of its tertiary structure. Previously, a minimal RMSf values observed in lid 1 residues of mutant G55Y in toluene at both temperatures could be inter-relate to the lack of RMSd changes. The key indicators to describe temperature-dependence in this cold-active lipases are through protein compactness and surface area solvent accessibility (SASA). H-bond networks are crucial for protein compactness and when these interactions broke at high temperature (causing structure flexibility), both R_g and SASA started to increase [35]. In Fig. 3 (B), mutants T52Y and G55Y exhibited low in R-gyration when

Table 3
Predicting effects of mutagenesis on lid 1 of AMS8 lipase.

Residues substitution	Secondary structure	Solvent accessibility (%)	Side-chain forming hydrogen bond	Protein stability free energy change (ΔΔG) in Kcal/mol)
T52Y	Alpha-helix	53.9 ➔ 42.5 (partially accessible)	Saturated ➔No H-bond	1.98 (Stabilizing, retain or improve activity)
G55Y	Alpha-helix	11.5 ➔ 34.6 (buried to partially accessible)	No H-bond ➔ No H-bond	4.78 (Highly stabilizing, negatively affect activity)

Web server, Site Directed Mutator (SDM) http://www-cryst.bioc.cam.ac.uk/~sdm/sdm.php

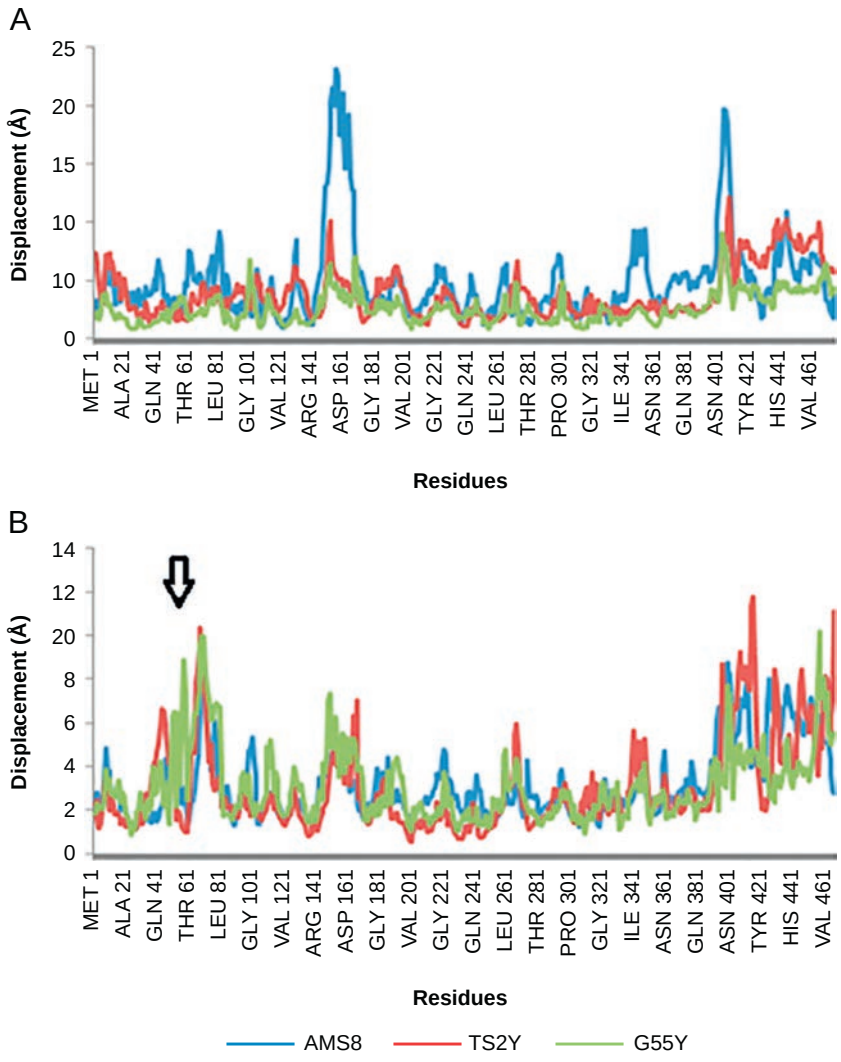

Fig. 1. Backbone Cα displacements of recombinant AMS8 and mutant lipases in molecular dynamics simulation with toluene at 25 °C (A) and 37 °C (B). Arrow points to the area where lid 1 is mainly located.

temperature was set at 37 °C. However, SASA values showed no difference in both temperatures (Fig. 3 (C)). Recombinant AMS8 lipase had the opposite trend at 37 °C, showing higher R-gyration and SASA values. Heat causes T52Y and G55Y structures to stabilize and settles at the point where proteins undergo less structural changes. Water clusters breaks apart, distributed across the protein conformation but the H_2O molecules should remain there. This analysis shows that mutations at lid 1 help to retain the H-bond interactions and water clusters surrounding enzyme surface.

3.3. Normal Mode Analysis (NMA) and Sequence-Specific Solvent Accessibilities (ProtSA) of Lid 1 Mutants

Normal mode analysis (NMA) is used to investigate collective motions and large-scale conformational transitions in proteins [36,37]. Apart from localized motions (detected by MD simulation), large-scale motions (detected by NMA) also play important role in the functional motions of an enzyme. According to matrix that compares 3 out of 5 modes of computed NMA analysis, recombinant AMS8 lipase has greater local flexibility at residues 140–170 specifically located at lid 2 regions (Fig. 4 A). In T52Y, 2 out of 5 modes were found to show greater Cα distance at residues 153–190 whereas in G55Y, 4 out of 5 modes were found to have largest fluctuated Cα distance starting from residues 48–59 and 162–172 (Fig. 4B and 4C). Gly-159 and Leu-163 exhibited largest increase in Cα distance by referring mutated Tyr-52 as a reference point. Leu-162 and Pro-168 were greatly distanced from Tyr-55 Cα backbone. These highly flexible residues were mostly found at lid 2. Based on the calculation of normal mode analysis, lid 2 and the C-terminal structure contributes greatly to the corresponding protein movement which was unlikely to occur with lid 1 even after sequence modification. Comparison of MD and NMA in toluene revealed that the overall protein conformation is identical for both recombinant and mutants. It was also observed that harmonic motion of lid 2 structure had been slightly disrupted by a single amino acid substitution of lid 1. Hence, lid 1 was not a focal site that able to influence the local flexibility of this protein.

There were two pre-indications that could define the overall role of lid 1 of AMS8 lipase after mutations. First, lid 1 did not participate in the process of interfacial activation. There was very little flexibility shown by this region in organic solvent and with increase of temperature [7,18]. This means, lid 1 would have existed as an imitation of a smaller lid which looks quite similar to lid 2 in *Pseudomonas sp.* MIS38 [10,38]. Secondly, the distance and coordination of active site residues were found to be greatly affected by lid 2 movements in the presence of toluene. The effects of mutations at residue Thr-52 and Gly-55 of AMS8 lipase showed a slight movement at lid 1 region and minimal disruption on lid 2 activation as the changes in folding by toluene causing the two lids to move against each other. Mutation that targets Thr-

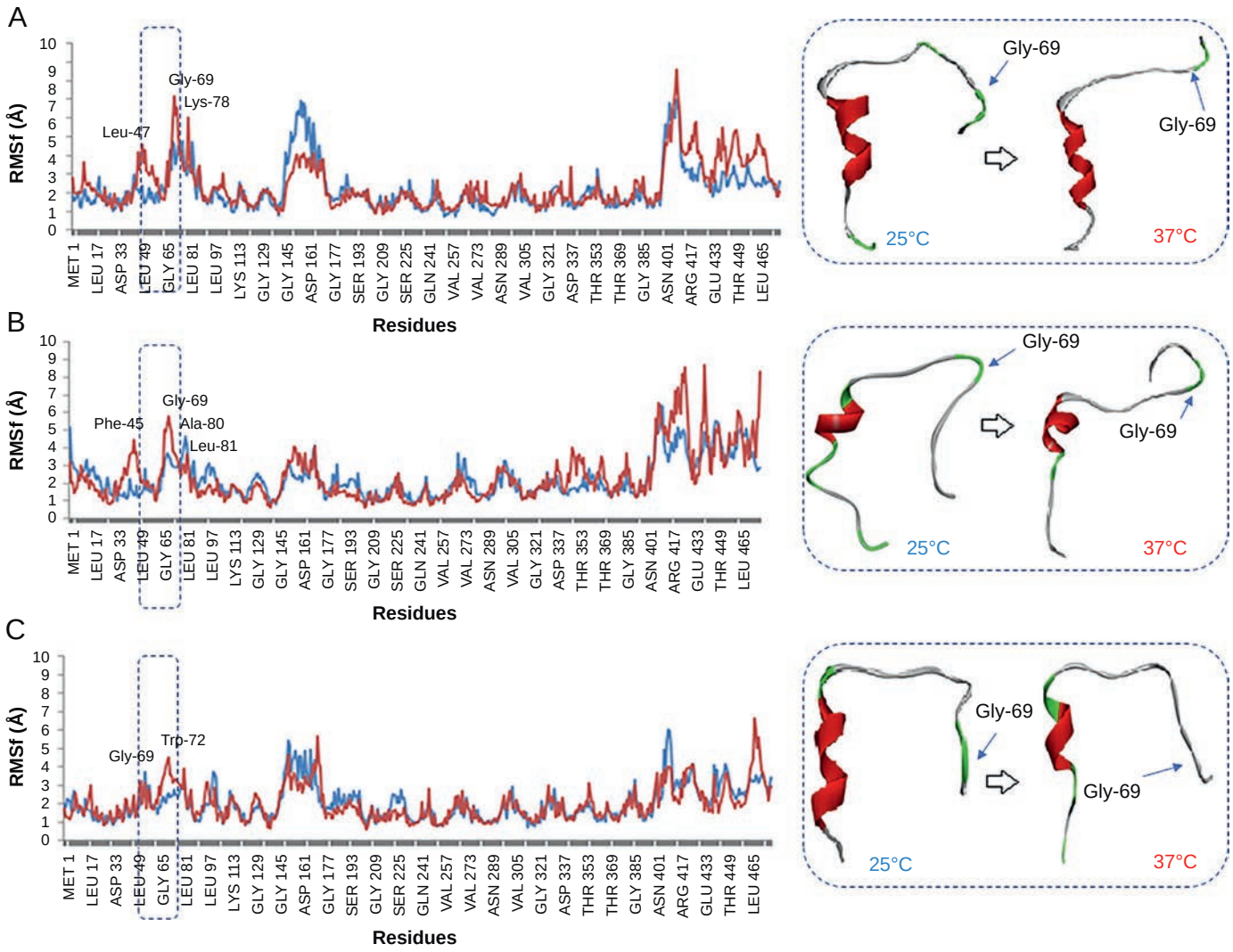

Fig. 2. Root-mean square fluctuation of recombinant lipase AMS8 (A), T52Y (B) and G55Y (C) in toluene simulated at 25 °C (blue line) and 37 °C (red line). Lid 1 and its nearby region (residues 49–70) were visualised in alpha-helix (red ribbon) surrounded by turns (green) and coils (grey). The location of Gly-69 was located at the hinge of lid 1 as shown on the right-hand side of this figure.

52 and Gly-55 on lid 1 confirmed the importance of this region to temperature stability subjected to biophysical changes. Altered optimal temperature, melting temperature, half-life and toluene stability was appropriate to describe the dependency of AMS8 lipase on the rigidity of lid 1. Molecular dynamics simulations at 37 °C showed that by mutating Thr-52 and Gly-55, the short lid 1 of AMS8 lipase may experience larger atomic movements. These movements were known to cause in regional flexibility of lid 1 without sacrificing much of the protein stability and was able to increase the solvent accessible surface area (ASA). Since the native state of protein can be recognized by losing the solvent accessible surface area (ASA), it was highly anticipated that the structural changes exhibited by these mutants at this temperature was contributed by protein folding [39]. One way to provide a realistic comparison of folding-unfolding state between mutants is through ProtSA, a web application that calculates sequence-specific solvent-accessibilities and the influence of point mutations on the protein stability [40]. Mutant T52Y and G55Y shared a number of 17 residues (which includes active site, Asp-255) identified to be within 45–90% of unfolded SASA whereas majority of residues were located within 90–110% of unfolded SASA. Mutant T52Y has a higher mean unfolded residue indicated by higher value in SASA as compared to G55Y (Fig. S1 and Table S1). Based on this output, ProtSA depicts that both mutated region of lid 1 appeared to gain a large percentage of solvent exposure upon mutation and was expected to destabilize the folded conformation of lid 1 when interacted with hydrophobic organic solvent. Hence, this data explained the actual indications of atomic movement involved residues from lid 1 and its surrounding during the molecular dynamics simulation in toluene.

3.4. Kinetic Outputs of Lid 1 Mutations Based on Small-, Medium- and Long-Substrate Length

Activation of lipase involves the displacement of the lid to expose the active site, suggesting that the dynamics of the lid could be of mechanistic and kinetic importance [41]. For recombinant AMS8 lipase, the positive changes in K_m had not resulted in any significant improvements to the k_{cat} and k_{cat}/K_m (Table 4). The k_{cat}/K_m in AMS8 lipase was meagrely raised in 0.5% (v/v) toluene in the presence of all three pNP substrates. G55Y was found to share similar preference with recombinant AMS8 in hydrolysing shorter pNP esters. Both recombinant and mutant G55Y lipases scored high k_{cat} and k_{cat}/K_m value following the low K_m observed for *p*NPC hydrolysis in 0.5% (v/v) toluene as shown in Table 4. Unlike these two lipases, mutant T52Y favours a longer chain carbon ester (*p*NPP) without the presence of toluene and shorter *p*NPC in 0.5% (v/v) toluene. The reason behind this change was probably due to the lowest total number of hydrogen bonds attained

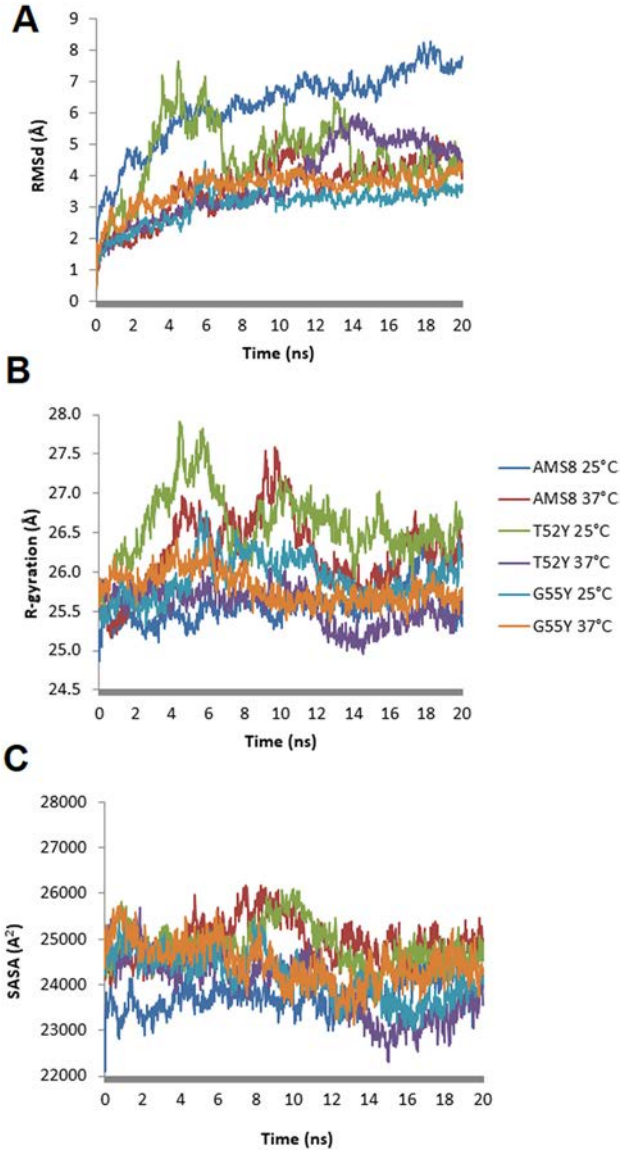

Fig. 3. A global backbone root-mean square deviations (A), R-gyration (B) and solvent accessible surface areas (SASA) (C) of recombinant AMS8, mutant T52Y and G55Y in toluene, equilibrated and simulated at 25 °C and 37 °C.

by mutant T52Y in water (9H-bonds) compared to recombinant AMS8 (12H-bonds) and G55Y (11H-bonds). The loss of hydrogen bond in T52Y makes the region slightly flexible and allows longer chain substrate to bind. The numbers of H-bond at lid 1 (highlighting residues 49–59) were all reduced in the presence of toluene as observed in the final simulation trajectories. This might be one of the reason in recombinant AMS8 to have improvements in K_m values at 0.5% (v/v) toluene. In T52Y and G55Y, the K_m improves across *p*NPC hydrolysis with 0–0.5% (v/v) toluene but not in *p*NPL and *p*NPP.

Albeit the improvement of mutant T52Y on substrate (*p*NPP) selectivity, the overall lipase activity and stability in 0.5% (v/v) toluene remained low in comparison to the recombinant. This suggests that mutation on lid 1 brings minor alteration in chain-length specificity and major changes towards molecular adaptations to organic solvent stability. Other similar cases involved substitutions of lid residues includes cold-adapted *Pseudomonas fragi* lipase (PFL). This study targets T137 and T138 located at lid domain to valine and asparagine, leading to successfully modified lipase chain-length preference profile by increasing the relative activity towards C-8 substrates [42]. A thermostable *Rhizopus chinensis* lipase (RCL) showed that by introducing a disulfide bond in the hinge of lid domain between F95C and F214C, the mutant RCLCYS had improved the K_m value of *p*NPP at 1.5 fold higher. However, RCLCYS preferred *p*NPA based on k_{cat}/K_m [29]. This mutation however did not convene to organic solvent adaptation properties.

The limitation of enzymatic catalysis in toluene could also be due to the implications of H-bond because the H-bonding process continuously competes with the presence of bulk water. This mechanistic insight suggested indiscriminate strengthening of H-bonds correlates poorly with experimental binding affinity [43]. Hence, an increase in H-bonds of lid 1 could interfere the binding of substrate due to the intensifying stability. Earlier in a closed-conformation of recombinant AMS8 lipase, there were a total of 17H-bond interactions found between residues 49 to 59 as shown in Table 2. After 20 ns simulation in toluene, the lipase exhibited reductions in the total number of H-bonds at similar area at 47% (Fig. 5A) When temperature was increased from 25 to 37 °C, the number of H-bonds lowered to 8 (53% reductions) where new H-bond interactions Ala-51-Leu-49, Leu-57-Val-54, Leu-58-Gly-55 and Ala-56-Leu-58 were formed (Fig. 5B). Other interactions were found preserved with increased in temperature. Based on this structures, lid 1 appeared rigid before simulations in toluene because of the interactions of H-bond between Thr-52 and Pro-68. The H-bond between Thr-52 and Pro-68 are found to be intact in lipase MIS38 and AMS8. Unlike in T52Y and G55Y lipase structures, this H-bond disappeared and left the coil structure to freely circumnavigate the lid domain. In T52Y, the hydrogen-bond interactions were reduced by 40% after underwent 20 ns of simulations in toluene at 25 °C. A few new H-bond interactions that appeared after 20 ns of simulation includes Gly-55-Tyr-52 and Gly-59-Ala-56(Fig. 5C). However, the H-bond networks changed at 37 °C when new bonds connecting Ala-51-Leu-49, Ala-56-Tyr-52, Gly-59-Gly-55 and Gly-59-Gly-55 were formed (Fig. 5D). This results indicated that mutation at Tyr-52 had a direct influence on the formation of H-bond at lid 1 through decline in its number from 10 to 6 at 25 °C. At 37 °C, the number of H-bonds were increased to strengthen alpha-helix structure. Both recombinant AMS8 and T52Y lipases exhibited higher flexibility at this area (Fig. 2A and B) due to the reorientation of the coil part which occurred in residues Gln-64 to Ile-70. Mutant G55Y exhibited growing numbers of hydrogen bonds between the residues 49 to 59 from 25 °C to 37 °C in toluene. In G55Y lipase, Tyr-55 formed hydrogen bonds with residues, Leu-58 and Gly-59 at 25 °C (Fig. 5E) whereas two more H-bonds formed with Thr-52 and Ser-60 at 37 °C which contributed to increase in rigidity of lid 1 structure (Fig. 5F). The coil and turns which creates the boundary of lid 1 in G55Y was pointing downwards showing lack of structure differences when being simulated at 37 °C. Compared to all mutant lipases, lid 1 from recombinant AMS8 lipase had the highest number of H-bonds that affect the degree of flexibility. By introducing hydrogen bond via tyrosine (a classic hydrogen bond donor) at residue 52 and 55 and subsequently interrupting other H-bonds at its area of vicinity, lid 2 flexibility comes to constraint in toluene. In this study, both alpha-helix lids from cold-active AMS8 lipase enthused a "see-saw" approach, showing its response to balance structural stability and flexibility. Based on this concept, there would hardly be a dual movement on two lids happened at the same time.

3.5. Biochemical and Biophysical Changes Following Lid 1 Mutations

In most lipases, reduced activity in organic solvent (in this case, toluene) was not always caused by protein denaturation due to organic solvent effects. It is more likely to happen because of the difference in half-life of enzyme in organic solvent [44]. The activating effects shown by recombinant AMS8 lipase in 0.5% (v/v) toluene verified that this cold-loving enzyme resist the presence of small amount of toluene which improves the K_m of pNP carbon-chain 8, 12 and 16 hydrolysis. The fact that toluene enhanced substrate binding defined the possibility on structural adaptation towards the presence of organic solvent during hydrolysis reactions. Because of toluene, this substrate finds its way to

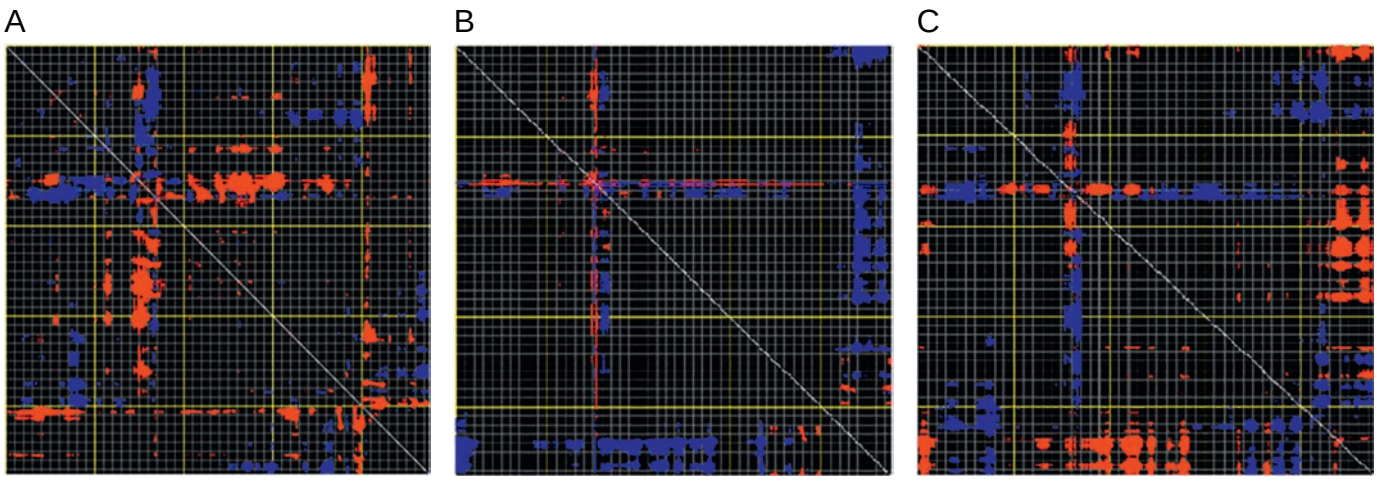

Fig. 4. Comparing one from five modes of distance fluctuation map of recombinant AMS8 (A), mutants T52Y (B) and G55Y (C) between all pairs of Cα atoms at the end simulation trajectories in toluene (25 °C). Distance increases of flexible blocks appeared in blue whereas decreases in distance of flexible regions are spotted in red. This matrix displays the maximum distance fluctuations attributed by the strongest 10% of the residue pair distance changes. Every pixel corresponds to a single residue. Grey lines are drawn for every 10 residues- and yellow lines for every 100 residues (counting from the upper left corner).

efficient binding with catalytic sites improving k_{cat} and k_{cat}/k_m of recombinant AMS8 lipase. Recombinant AMS8 lipase was found to be highly stable and active at optimal temperature of 45 °C as shown in Table 5.

Other mutants featured on lid area such as T52Y shared optimal temperature with G55Y via significant reduction of 10 °C temperature. Half-life of T52Y was longer at 25 °C (> 10 h) without toluene but shorter in 0.5% (v/v) toluene (8 h). When temperature was increased to 37 °C, the half-life of mutant T52Y declined but remained active at half its activity up to 9 h without toluene and 5 h with 0.5% (v/v) toluene. The low substrate affinity (higher K_m) of T52Y in 0.5% (v/) toluene in pNP-palmitate could share similar trends to its affinity in a long-chain fatty acid substrate, olive oil at 25 °C because of its longer half-life. The half-life trend at 0.5% (v/v) toluene however was shorter in G55Y. At 25 °C, mutant G55Y achieved longer-half-life in 0.5% (v/v) toluene but shorter in toluene-free hydrolysis reaction. As temperature increased, G55Y half-life dropped at 1.5 h in which toluene did not set to improve its half-life at 37 °C, similar to the rest of lipases. Apparently, thermal stability of T52Y and G55Y was very much declined by the reducing half-life in 0.5% toluene as compared to parent lipase. In other study, lid mutants of cold-adapted *Pseudomonas fragi* lipase (PFL) exhibited thermal stability following the time-dependent loss of activity at 29 °C, a temperature where subtle changes in stability can be observed [42]. Parent lipase (PFL) on tricaprylin was found reduced by 50% after 4 h incubation, whereas, under the same conditions, mutant T137 V still retained 90% of its activity and mutant T138 N remained active at 70%.

Given a range of toluene concentrations (0–10%, v/v), most lipases exhibited tolerance at 1–3% (v/v) toluene (Fig. S2). Because all lipases expressed high stability and activity at low concentration of toluene, a decline on conformational stability would be expected at any concentration of toluene exceeding 3% (v/v). This might be due to the relatively high viscosity of the solvents, which hindered efficient interaction between the enzymes and substrates [44]. Based on widely reported scientific evidence, toluene is considered highly toxic to most microorganisms and enzymes secreted by them even though being exposed at lowest toluene concentration of 0.1% (v/v) [45].

Aggregation and precipitation (Fig. S3) of protein mostly occurred due to the exposure of protein in incompatible solvent [46]. In all lipases studied, denaturation precedes aggregation in toluene showing that aggregate protein may also exhibited partially denatured state. Without toluene, the aggregation points appeared before denaturation. Both circumstances placed recombinant AMS8 and lid 1 mutant lipases at different state of folding/unfolding. Through this, toluene was depicted as a driving-force in supporting the progression of protein folding and minimizing structure instability when it comes to high temperature. For lid 1 mutants, the outcome of melting temperature suggested different verdicts on the progression of protein denaturation in the presence of toluene. Mutant G55Y showed to exhibit melting point (T_m) of 60.01 °C whereas T52Y T_m was slightly lower at 57.38 °C. In toluene, both

Table 4
Michaelis Menten kinetics measuring K_m and k_{cat} of mutants T52Y and G55Y. Three types of pNP substrates were used in kinetic study at 25 °C, stated as A, B and C, where A signifies pNP palmitate (C-16), B for pNP laurate (C-12) and C for pNP caprylate (C-8).

	WT AMS8		T52Y		G55Y	
	0% toluene (v/v)	0.5% toluene (v/v)	0% toluene (v/v)	0.5% toluene (v/v)	0% toluene (v/v)	0.5% toluene (v/v)
K_m (mM)	A: 2.59 ± 2.7	A: 0.79 ± 0.1	A: 32.47 ± 5.1	A: 45.92 ± 6.1	A: 7.11 ± 6.4	A:80.53 ± 74.4
	B: 1.85 ± 2.9	B: 0.69 ± 0.3	B: 48.17 ± 0.0	B: 45.45 ± 9.3	B: 15.58 ± 19.3	B:18.32 ± 0.5
	C: 0.73 ± 2.0	C: 0.63 ± 0.7	C: 59.63 ± 18.8	C. 27.42 ± 2.46	C: 7.19 ± 4.9	C: 3.83 ± 0.7
k_{cat} (S^{-1})	A: 2.16×10^{-7}	A: 5.02×10^{-6}	A: 6.51×10^{-7}	A: 3.11×10^{-6}	A: 7.59×10^{-6}	A: 4.14×10^{-5}
V_{max}/[ET]	B: 1.86×10^{-7}	B: 5.13×10^{-6}	B: 1.01×10^{-5}	B: 1.44×10^{-5}	B: 4.34×10^{-5}	B: 5.47×10^{-5}
	C: 2.87×10^{-7}	C: 1.97×10^{-5}	C:2.14×10^{-5}	C: 2.97×10^{-5}	C: 4.80×10^{-6}	C: 2.12×10^{-5}
k_{cat}/K (mM^{-1} S^{-1})	A: 8.37×10^{-8}	A: 6.92×10^{-6}	A: 2.00×10^{-8}	A: 6.77×10^{-8}	A. 1.06×10^{-6}	A. 5.14×10^{-7}
	B: 1.01×10^{-7}	B: 7.44×10^{-6}	B: 2.09×10^{-7}	B: 3.17×10^{-7}	B. 2.78×10^{-6}	B. 2.98×10^{-6}
	C: 3.93×10^{-7}	C: 1.56×10^{-4}	C: 3.59×10^{-7}	C: 1.08×10^{-6}	C: 6.67×10^{-7}	C: 5.53×10^{-6}

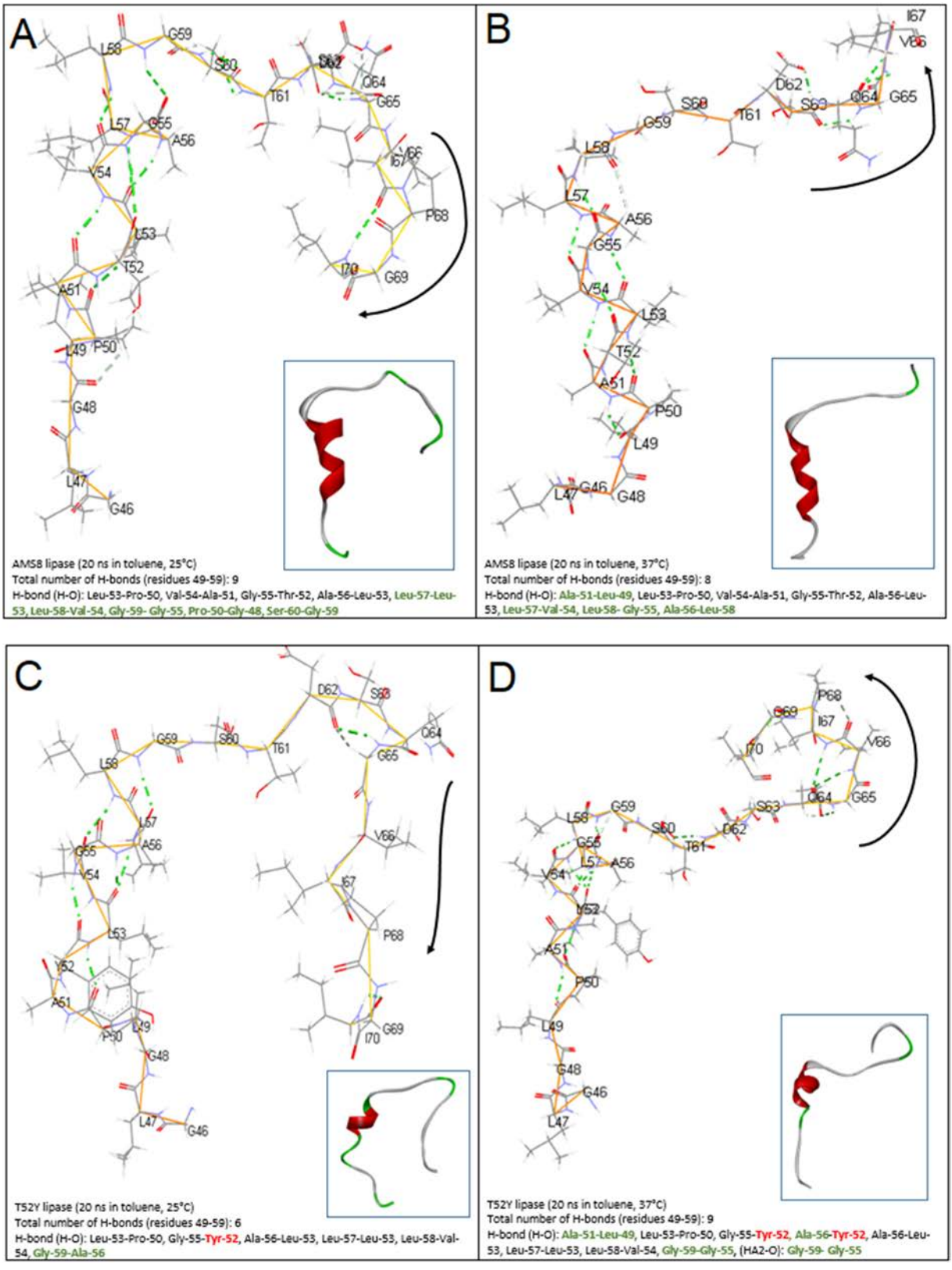

Fig. 5. Hydrogen bond interactions at Thr-52 and Gly-55 in recombinant AMS8 (A, B), T52Y (C, D) and G55Y (E, F) in toluene. Lid 1 structures (highlighting residues 46–70) showed the structure at 25 °C (A, C and E) and 37 °C (B, D and F) simulation in toluene. The helix structure of lid 1 was presented in red colored ribbon. The pointing arrow indicates the direction in hinge movements coordinated by turns (shown in green ribbon) and coil structure (grey ribbon). H-bonds are shown in green-lines connecting residues at 49–59, revealing the total numbers of H-bond interactions within this area. In the list of H-bond interactions, the mutated residues (with H-bond) are highlighted in red font and new H-bond interactions (which exclusively appeared in either 25 or 37 °C) are differentiated by green font.

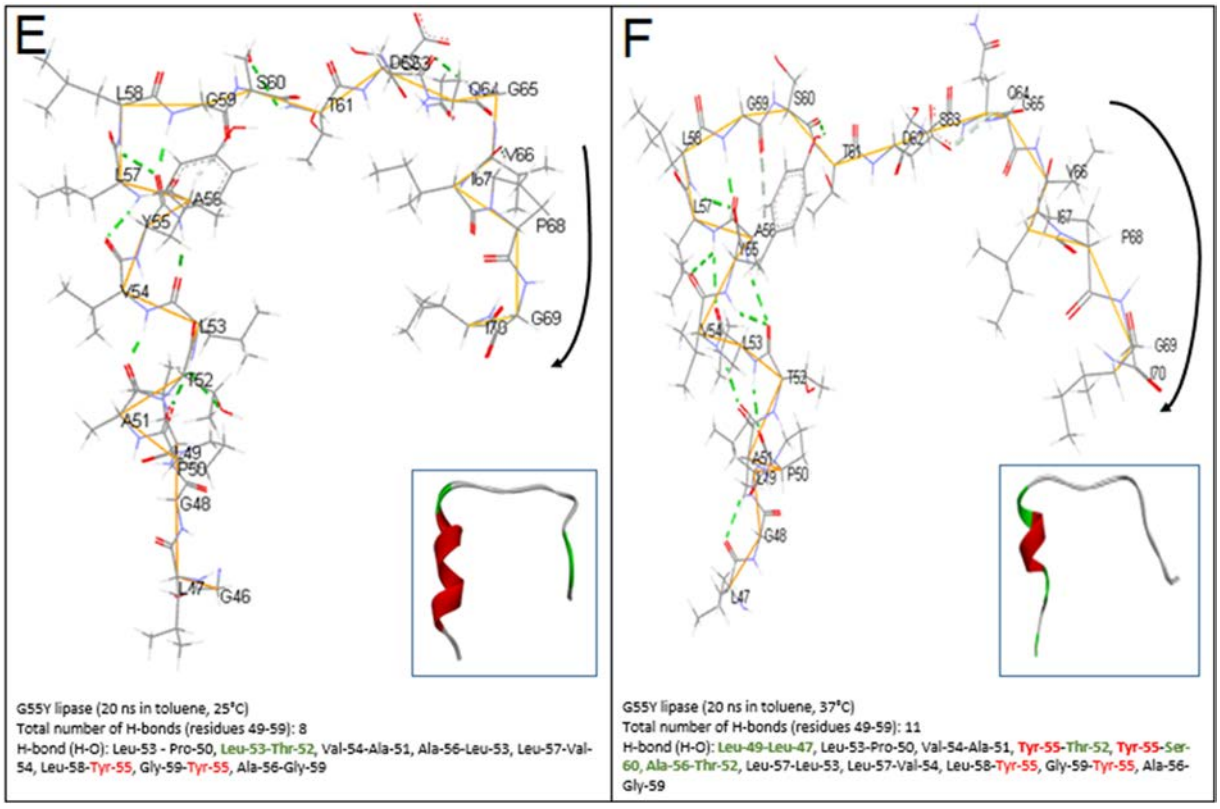

Fig. 5 (*continued*).

mutants T_m dropped to 46.5 °C showing their higher tendency of protein denaturation. A decline in denaturation point of T52Y and G55Y mutants at 2% (v/v) toluene illustrates the weakening of hydrophobic interactions among buried residues. As a consequence of this situation where more buried peptide groups and side chains are exposed to solvent, the tightly packed non-polar side chain and peptide groups are getting reduced in number. Losing the intramolecular hydrogen bonds required for buried residues exposes the packing of close-packed spheres and groups in the interior of a protein to protein unfolding or denaturation [47]. The denatured states of cold-active protein can be understood from the increased formation of randomly coiled structure. Thus, it is clear that two important conditions must be met by lipase to co-exist in a solvent, in which firstly, the native state of protein must be favored and second, protein must be active and soluble in its optimum concentration of solvent.

3.6. Thermodynamic Profiles of Lid 1 Mutants in Toluene

The difference of energy states for converting reactant into product can be determined by using ΔG, ΔH and ΔS. Gibbs free energy describes the capacity of a thermodynamic system to do maximum or reversible work at a constant temperature and pressure. It is said that negative ΔG is obtained when the system reaches an equilibrium state at constant pressure and temperature, but a fast drop in ΔG will also indicates a sign of protein denaturation [48]. In this study, all lipases generally exhibited decline in ΔG after temperature was switched from 25 °C to higher temperature (35 °C) in the presence of 0.5% (v/v) toluene (Table 6). Through the negative changes of free energy, these lid 1 mutants and parent AMS8 lipases were thermodynamically driven and act as biocatalyst under a spontaneous reaction to form product [49] as ΔG can tell the difference of energy between reactants and products. Compared to recombinant AMS8, all mutants exhibited lower ΔG‡ values in toluene and without 0.5% (v/v) toluene at both temperatures. This finding suggested that lid 1 mutants could display higher catalytic rate in response to the rise in temperature regardless in which system. Subsequently, ΔG‡ values can be use in determining the stability of protein-substrate complex in toluene based on the enthalpy-entropy balance. The cold-adapted enzymes invariably show a more negative entropy and a lower enthalpy of activation than their mesophilic orthologs [50].

Enthalpy is a measure of total energy of a thermodynamic system in which higher enthalpy shows lower catalytic rates at respective temperature [48]. Most of lipases exhibited decline in ΔH‡ when measured from 25 °C to 35 °C with and without 0.5% (v/v) toluene. Low ΔH‡ value in mutant G55Y indicates that this mutant has higher catalytic rates for *p*NPC hydrolysis in toluene. Since k_{cat} was measured based on its reaction to smaller-chain substrate (*p*NPC) in toluene, this result confirmed that the enthalpy changes not only caused by differences in temperature but also due to its association with substrate specificity. In reaction without toluene, recombinant AMS8 was found to exhibit higher catalytic rate due to low ΔH‡ followed by T52Y. In this study, recombinant AMS8 and T52Y lipases were found to have catalytic inefficiencies when used for catalysis in toluene and this was shown via the decline in k_{cat}. Nonetheless, the activity improved when the lipases were used in toluene-free reaction.

Entropy is a measure of distributed heat energy over the thermodynamic system. Heat always flows from regions of higher temperature to regions of lower temperature with its positive and negative signs indicating the overall increase and decrease in degree of the freedom of the system, respectively [48]. The increase in negative entropy will or might lead to further instability of protein creating a softer structure. This corresponds to the entropic effects commonly found in enzymes that are adapted by evolution to work at low temperatures [50]. Mutant T52Y was found to have a slight increase of ΔS‡ value from 25 °C to 35 °C in 0.5% (v/v) toluene indicating lower degree of structure disorder whereas the other lipases did not show changes in structure disorder at these temperatures. On this basis, mutant T52Y was found to be

Table 5
Biophysics and biochemical properties of mutants T52Y and G55Y.

	Recombinant AMS8	T52Y	G55Y
1. Changes of secondary structure following increase in temperature 20–30 °C	decrease α-helix, increase random coil	Increase random coil	Decrease α-helix, increase random coil
2. Optimal temperature (°C)	45 (± 0.04)	35 (± 0.01)	35 (± 0.06)
3. Half-life at 25 °C (min)			
a) without toluene	300 (5 h)	>600 (> 10 h)	150 (2.5 h)
b) with 0.5% (v/v) toluene	300 (5 h)	480 (8 h)	210 (3.5 h)
4. Half-life at 37 °C (min)			
a) without toluene	300 (5 h)	540 (~ 9 h)	90 (1.5 h)
b) with 0.5% (v/v) toluene	300 (5 h)	300 (5 h)	90 (1.5 h)
5. Stability in toluene (v/v, %) at 25 °C (range of concentration 0–10 v/v, %)	1	3	3
6. Aggregation point, T_{agg} (°C) by DLS			
a) Without toluene	35	40	50
b) 0.5% (v/v) toluene	62.5	50	50
7. Denaturation point, T_m (°C) by CD			
a) Without toluene	45.8	57.38	60.01
b) 2% (v/v) toluene	53.5	46.6	46.5

Notes: Differences in toluene concentration measured for T_{agg} and T_m in DLS and CD are based on the allowed detection limit in respective equipment. Ideal concentration of non-polar solvent in CD was identified at 0.5–5% (v/v) and 0.5–1% (v/v) in dynamic light scatterings (DLS) when performed under gradually increased temperature 20–80 °C. All assays were performed in 3-replicates (± standard deviation).

thermodynamically stable in the presence of toluene. As for enthalpy-entropy equilibrium in toluene, T52Y exhibited high enthalpy with increasing entropy. This result was an indication of a functionally compromised (reducing rate of activity) but stable lipase. In a normal system (a reaction without toluene), G55Y showed the highest enthalpy of activation, $\Delta H^{\ddagger}$ a sign where more energy is required for the products to form (substrate turnover). The high enthalpy value was followed with increase in entropy, $\Delta S^{\ddagger}$ that further intensify protein stability. As a consequence of these analysis, it was found that temperature is a good precursor to determine the stability of AMS8 lipase and lid 1 mutants as well as the extent of their activity. In this study, toluene facilitates stability and activity of lid 1 mutant T52Y through its improvement from structure disorder (high entropy) thus reducing its catalytic rate (k_{cat}) via high enthalpy.

Optimum temperature for recombinant AMS8 was found to be 45 °C while lid 1 mutants exhibited significantly lower in optimum temperature. Therefore, by logic these mutants should displayed loss of catalytic activity/rate if reaction do takes place at temperature higher than 35 °C. In order to relate the effects of catalytic activity with changes in temperature, activation energy was measured using the k_{cat} value of individual reactions in separate temperature. In this analysis, activation energy was found to be very much affected with increase in temperature especially in recombinant AMS8. However technically, some had indicated that with higher temperature the plot would not be suitable in measuring the activation energy as it might illustrate the inactivation of its function by losing its activity corresponded to a decline in k_{cat} values (Fig. S4). By varying the rate constant with changing temperatures, the Activation Energy (Ea) could be determined. Ea is the energy level that the reactant molecules must overcome before a reaction can occur. Hence, higher activation energy (Ea) signifies slower in catalytic rate and substrate turnover. The value can be estimated via the slope of Arrhenius plot (ln k_{cat} plots against 1/T) (Fig. S4) or by using formula (Eq. 1). Since the determination of Ea via slope was difficult due to the relatively flat slope in its reaction with toluene, the Ea was measured by using formula (1). In free-solvent system, the rate of *p*NPC hydrolysis decreased with increased in temperature (25 °C to 35 °C). The decline in k_{cat} values resulted in increased of activation energy in recombinant AMS8 and T52Y at 0.5% (v/v) toluene according to Table 7. Only G55Y lipase showed negative activation energy in the presence of 0.5% (v/v) toluene. Without toluene, both recombinant AMS8 and T52Y lipases achieved higher catalytic rate at 25–35 °C. As a conclusion, the hydrolysis of *p*NPC in T52Y and parent lipases were activated and catalytically more efficient in solvent-free system compared to reactions in toluene.

The reason to cold-active lipase having slower reactions at higher temperature could be supported by two contributing factors. Firstly, an increase in temperature shifts equilibria in favor of their endothermic reaction. This means a reverse direction of the first step from A + B ➔ C to C ➔ A + B was implicated. Hence, the rate law had switched from $v_1 = k_1[A][B]$ to $v_{-1} = k_{-1}[C]$ giving a negative Arrhenius expression. Secondly, the rate coefficients or k_{cat} might have altered at higher temperatures through the antagonism of two steps which happens at the same time, A + B➔C (step 1) and C➔P (step 2). Thus, based on these factors, this reaction was enthalpically favored over return to reactants [51]. In much simple conjecture, higher temperature makes substrate

Table 6
Thermodynamics parameters of recombinant AMS8 and lid 1 mutant lipases, T52Y and G55Y with and without 0.5% (v/v) toluene. All thermodynamic values were derived based on the independent calculations of k_{cat} on temperatures (25° and 35 °C) by using eqs. 2, 3 and 4.

Temperature (°C)		Gibbs Free Energy of Activation Energy, $\Delta G^{\ddagger}$ (kJ/mol)		Enthalpy, $\Delta H^{\ddagger}$ (kJ/mol)		Entropy, $\Delta S^{\ddagger}$ (kJ/mol)	
		0.5% (v/v) Toluene	No toluene	0.5% (v/v) Toluene	No toluene	0.5% (v/v) Toluene	No toluene
25	WT	−113.98	−119.62	101.74	−144.21	0.72	−0.08
	T52Y	−114.63	−120.72	312.23	−39.31	1.43	0.27
	G55Y	−121.19	−118.26	−50.20	112.63	0.24	0.77
35	WT	−121.22	−118.78	101.65	−144.29	0.72	−0.08
	T52Y	−151.56	−121.58	312.15	−39.40	1.53	0.27
	G55Y	−123.55	−126.00	−50.29	112.55	0.24	0.77

Table 7
Estimated activation energy in kJ/mol derived from aforementioned Eq. 1. Formula used to calculate was slope = −Ea/R where R is a constant equal to 8.314 J/molK^{-1} using temperature 25 °C to 35 °C.

	0.5% (v/v) toluene	Without toluene
Recombinant	104	−142
T52Y	314	−36.834
G55Y	−47	115.11

difficult to bind to the active site which results in a drop of reaction constant (k_{cat}).

4. Conclusion

The effects of mutations at residue Thr-52 and Gly-55 of AMS8 lipase showed a slight movement at lid 1 region and minimal disruption on lid 2 activation. Mutation that targets T52Y and G55Y on lid 1 confirmed on the importance of this region to temperature stability according to the results of biophysical analysis and molecular dynamics simulations. Analysis on the altered optimal temperature, melting temperature, half-life and toluene stability clearly described the dependency of AMS8 lipase structure stability on the rigidity of lid 1. As an added advantage to these work, mutant T52Y showed preference to the long carbon-chain substrate or, *p*NPP-16 via Michaelis-Menten constant (K_m) which seems to support hydrolysis without toluene at 25 °C. This mutant however continued to fancy hydrolysis of smaller-chain pNP (*p*NPC) in 0.5% (v/v) toluene. In 0.5% (v/v) toluene, catalytic efficiency of G55Y is higher than T52Y in 2 out of 3 substrates tested. Mutants T52Y and G55Y unfold faster in 2% toluene than without solvent. Analysis on protein denaturation profiles was found not to be correlated with increase in toluene concentrations. Both enthalpy and entropy exhibited decline in value indicated high catalytic activity and higher degree of structure loss when toluene was added. All lipases exhibited decline in Gibbs free energy and $\Delta H‡$ when measured from 25 °C to 35 °C in 0.5% (v/v) toluene. There was least change occurred to $\Delta S‡$ between these temperatures. Therefore, *p*NPC hydrolysis in mutant lid 1 lipases showed to have higher catalytic rate in toluene between 25 and 35 °C. Instead of temperature, the structure loss was very much dependent on the toluene concentration. The enzyme will become a highly relevant industrial biocatalyst if it is able to utilize broad catalysis reactions at low and moderate temperature. For now, lid 1 has shown to be the epitome of AMS8 lipase structure stability. Previously, the same cold-active recombinant AMS8 lipase has demonstrated maximum yield for ester conversion at 20 °C for a short period where 62% ester conversion was found in toluene and 47% in hexane. This yield was higher than reactions without organic solvents (35%). This means, the conversion percentage of ethyl hexanoate was significantly improved in the presence of toluene compared to other organic solvents and solvent-free system [52]. Our views in improving the esterification yield is by achieving higher solvent-accessibility via lid 1 surface engineering.

Author Contributions

All authors reviewed the manuscript. N.Y. and M.S.M.A designed the experiments. N.Y. conducted all experiments. N.Y analysed all data, performed data curation wrote and revised the manuscript. M.S.M.A involved in proof-reading the manuscript, project management and funding. A.T.C.L. contributed to the software for molecular dynamics simulation (YASARA version 11.3.22). N.H.A.K., A.T.C.L, A.B·S, R.N.Z.R.A.R and M.S.M.A were the Principal Investigators of Enzyme and Microbial Technology Research Centre whom contributed equally in research discussion, instrumentations, purchasing of reagents and chemicals. All authors read and approved the final manuscript.

Funding

This research was funded by Putra Graduate Initiative (IPS), Universiti Putra Malaysia with grant number 9536300. N.Y. was a recipient of Graduate Research Fellowship (GRF) scholarship awarded by School of Graduate Studies, Universiti Putra Malaysia.

Conflicts of Interest

There was no conflict of interest. The funder had no role in the design of the study; in the collection, analyses, or interpretation of data; in the writing of the manuscript, or in the decision to publish the results.

Appendix A. Supplementary data

Supplementary materials: Fig. S1: The relation (in percentage) between the unfolded SASA of the individual residues of T52Y (A) and G55Y (B) and that of the average unfolded SASA for that residue type for a test set of 19 other proteins, Fig. S2: Toluene stability analysis based on toluene concentration (0, 1, 3, 5, 7, 10%), Fig. S3: Aggregation point (or tendency to oligomerize/ aggregate) found in purified protein of recombinant AMS8 (A, B), T52Y (C, D), and G55Y (E, F) with and without 0.5% (v/v) toluene, Fig. S4: Arrhenius plot with calculated ln k_{cat} and 1/T (K^{-1}) to estimate the value of activation energy (Ea) of the system, Table S1: Mean and total unfolded residue of SASA obtained at Thr-52 and Gly-55 from recombinant (WT) AMS8, Tyr-52 from mutant (Mut T52Y) and Tyr-55 from mutant (Mut G55Y). Supplementary data associated with this article can be found in the online version, at doi:https://doi.org/10.1016/j.csbj.2019.01.005.

References

[1] Lan D, Wang Q, Popowicz GM, Yang B, Tang Q, Wang Y. The role of residues 103,104 and 278 on the activity of SMG1 lipase from *Malassezia globosa*: a site-directed mutagenesis studies. J Microbiol Biotechnol 2015;25:1827–34. https://doi.org/10.4014/jmb.1506.06079.
[2] Houde A, Kademi A, Leblanc D. Lipases and their industrial applications: an overview. Appl Biochem Biotechnol 2004;118:155–70. https://doi.org/10.1385/ABAB:118:1-3:155.
[3] Zhang X-F, Yang G-Y, Zhang Y, Xie Y, Withers SG, Feng Y. A general and efficient strategy for generating the stable enzymes. Sci Rep 2016;6(1–12). https://doi.org/10.1038/srep33797.
[4] Skjold-Jørgensen J, Vind J, Svendsen A, Bjerrum MJ. Lipases that activate at high solvent polarities. Biochemistry 2016;55:146–56. https://doi.org/10.1021/acs.biochem.5b01114.
[5] Secundo F, Carrea G, Tarabiono C, Gatti-Lafranconi P, Brocca S, Lotti M, et al. The lid is a structural and functional determinant of lipase activity and selectivity. J Mol Catal B: Enzym 2006;39:166–70. https://doi.org/10.1016/j.molcatb.2006.01.018.
[6] Brocca S, Secundo F, Ossola M, Alberghina L, Carrea G, Lotti M. Sequence of the lid affects activity and specificity of *Candida rugosa* lipase isoenzymes. Protein Sci 2003;12:2312–9. https://doi.org/10.1110/ps.0304003.
[7] Ali MSM, Fuzi SFM, Ganasen M, Rahman RZRA, Basri M, Salleh AB. Structural adaptation of cold-active RTX lipase from Pseudomonas sp. strain AMS8 revealed via homology and molecular dynamics simulation approaches. Biomed Res Int 2013;2013:1–9. https://doi.org/10.1155/2013/925373.
[8] Faraggi E, Zhou Y, Kloczkowski A. Accurate single-sequence prediction of solvent accessible surface area using local and global features. Proteins 2014;82:3170–6. https://doi.org/10.1002/prot.24682.
[9] Khan FI, Lan D, Durrani R, Huan W, Zhao Z, Wang Y. The Lid Domain in Lipases: Structural and Functional Determinant of Enzymatic Properties. Front Bioeng Biotechnol 2017;5:1–13. https://doi.org/10.3389/fbioe.2017.00016.
[10] Angkawidjaja C, You DJ, Matsumura H, Kuwahara K, Koga Y, Takano K, et al. Crystal structure of a family I.3 lipase from Pseudomonas sp. MIS38 in a closed conformation. FEBS Lett 2007;581:5060–4. https://doi.org/10.1016/j.febslet.2007.09.048.
[11] Korman TP, Bowie JU. Crystal structure of *Proteus mirabilis* lipase, a novel lipase from the proteus/psychrophilic subfamily of lipase family I.1. PLoS One 2012;7:1–8. https://doi.org/10.1371/journal.pone.0052890.
[12] Jeong ST, Kim HK, Kim SJ, Chi SW, Pan JG, Oh TK, et al. Novel zinc-binding center and a temperature switch in the *Bacillus stearothermophilus* L1 lipase. J Biol Chem 2002;277:17041–7. https://doi.org/10.1074/jbc.M200640200.
[13] Pandurangan AP, Ochoa-Montaño B, Ascher DB, Blundell TL. SDM: a server for predicting effects of mutations on protein stability. Nucleic Acids Res 2017;45:W229–35. https://doi.org/10.1093/nar/gkx439.

[14] Ali MSM, Ganasen M, Rahman RNZRA, Chor ALT, Salleh AB, Basri M. Cold-adapted RTX Lipase from Antarctic *Pseudomonas* sp. Strain AMS8: Isolation, Molecular Modeling and Heterologous Expression. Protein J 2013;32:317–25. https://doi.org/10.1007/s10930-013-9488-z.
[15] Ganasen M. Expression and characterization of a cold-adapted lipase from an Antarctic *Pseudomonas sp*. Master Thesis Malaysia: Universiti Putra Malaysia; 2014.
[16] Laemmli UK. Cleavage of structural proteins during the assembly of the head of bacteriophage T4. Nature 1970;277:680–5. https://doi.org/10.1038/227680a0.
[17] Bradford MM. A rapid and sensitive method for the quantitation of microgram quantities of protein utilizing the principle of protein-dye binding. Anal Biochem 1976; 72:248–54. https://doi.org/10.1006/abio.1976.9999.
[18] Yaacob N, Ali MSM, Salleh AB, Rahman RNZRA, Leow ATC. Toluene promotes lid 2 interfacial activation of cold-active solvent tolerant lipase from *Pseudomonas fluorescens* strain AMS8. J Mol Graph Model 2016;68:224–35. https://doi.org/10.1016/j.jmgm.2016.07.003.
[19] Alexandrov V, Lehnert U, Echols N, Milburn D, Engelman D, Gerstein M. Normal modes for predicting protein motions: a comprehensive database assessment and associated Web tool. Protein Sci 2005;14:633–43. https://doi.org/10.1110/ps.04882105.
[20] Estrada J, Bernadó P, Blackledge M, Sancho J. ProtSA: a web application for calculating sequence specific protein solvent accessibilities in the unfolded ensemble. BMC Bioinform 2009;10:1–8. https://doi.org/10.1186/1471-2105-10-104.
[21] Kwon DY, Rhee JS. A simple and rapid colorimetric method for determination of free fatty acids for lipase assay. J Am Oil Chem Society 1986;63:89–92. https://doi.org/10.1007/BF02676129.
[22] Dror A, Shemesh E, Dayan N, Fishman A. Protein engineering by random mutagenesis and structure-guided consensus of *Geobacillus stearothermophilus* lipase T6 for enhanced stability in methanol. Appl Environ Microbiol 2014;80:1515–27. https://doi.org/10.1128/AEM.03371-13.
[23] Raussens VI, Ruysschaert JM, Goormaghtigh E. Protein concentration is not an absolute prerequisite for the determination of secondary structure from circular dichroism spectra: a new scaling method. Anal Biochem 2003;319:114–21. https://doi.org/10.1016/S0003-2697(03)00285-9.
[24] Truongvan N, Jang S-H, Lee CW. Flexibility and stability trade-off in active site of cold-adapted *Pseudomonas mandelii* Esterase EstK. Biochemistry 2016;55:3542–9. https://doi.org/10.1021/acs.biochem.6b00177 1-29.
[25] Prajapati V, Patel H, Trivedi U, Patel K. Kinetic and thermodynamic characterization of lipase produced by *Cellulomonas flavigena* UNP3. J Basic Microbiol 2014;54: 976–83. https://doi.org/10.1002/jobm.201300065.
[26] Sharma A, Dalai AK, Chaurasia SP. Thermodynamic study of hydrolysis and esterification reactions with immobilized lipase. Eur Int J Sci Technol 2015;4:128–36 ISSN: 2304-9693.
[27] Andualema B, Gessesse A. Microbial lipases and their Industrial applications: review. Biotechnology 2012;11:100–18. https://doi.org/10.3923/biotech.2012.100.118.
[28] Cheng M, Angkawidjaja D, Koga Y, Kanaya S. Requirement of lid 2 for interfacial activation of a family I.3 lipase with unique two lid structures. FEBS J 2012;279: 3727–37.
[29] Yu X-W, Tan N-J, Xiao R, Xu Y. Engineering a disulfide bond in the lid hinge region of *Rhizopus chinensis* Lipase: increased thermostability and altered acyl chain length specificity. PLoS One 2012;7:1–7. https://doi.org/10.1371/journal.pone.0046388.
[30] Magliery TJ. Protein stability: computation, sequence statistics, and new experimental methods. Curr Opin Struct Biol 2015;33:161–8. https://doi.org/10.1016/j.sbi.2015.09.002.
[31] Timucin E, Sezerman OU. The conserved lid tryptophan, W211, potentiates thermostability and thermoactivity in bacterial thermoalkalophilic lipases. PLoS One 2013; 8:1–17. https://doi.org/10.1371/journal.pone.0085186.
[32] Hamid THA, Rahman RNZRA, Salleh AB, Basri M. The role of lid in protein-solvent interaction of the simulated solvent stable thermostable lipase from *Bacillus* Strain 42 in water-solvent mixtures. Biotechnol Biotechnol Equip 2009;23:1524–30. https://doi.org/10.2478/V10133-009-0015-5.
[33] Willems N, Lelimousin M, Koldsø H, Sansom MSP. Interfacial activation of M37 lipase: a multi-scale simulation study. Biochim Biophys Acta 2017;1859:340–9. https://doi.org/10.1016/j.bbamem.2016.12.012.
[34] Skjold-Jørgensen J, Vind J, Svendsen A, Bjerrum MJ. Altering the activation mechanism in *Thermomyces lanuginosus* Lipase. Biochemistry 2014:1–9. https://doi.org/10.1021/bi500233h.
[35] Brovchenko I, Andrews MN, Oleinikova A. Thermal stability of the hydrogen-bonded water network in the hydration shell of islet amyloid polypeptide. J Phys Condens Matter 2011;23:1–9. https://doi.org/10.1088/0953-8984/23/15/155105.
[36] Dobbins SE, Lesk VI, Sternberg MJE. Insights into protein flexibility: the relationship between normal modes and conformational change upon protein–protein docking. PNAS 2008;105:10390–5. https://doi.org/10.1073/pnas.0802496105.
[37] Suhre K, Sanejouand YH. ElNemo: a normal mode web server for protein movement analysis and the generation of templates for molecular replacement. Nucleic Acids Res 2004;32:W610–4. https://doi.org/10.1093/nar/gkh368.
[38] Angkawidjaja C, Matsumura H, Koga Y, Takano K, Kanaya S. X-ray Crystallographic and MD simulation Studies on the Mechanism of Interfacial Activation of a Family I.3 Lipase with two lids. J Mol Biol 2010;400:82–95. https://doi.org/10.1016/j.jmb.2010.04.051.
[39] Lu S, Wagaman AS. On methods for determining solvent accessible surface area for proteins in their unfolded state. BMC Res Notes 2014;7:1–7. https://doi.org/10.1186/1756-0500-7-602.
[40] Estrada J, Bernadó P, Blackledge M, Sancho J. ProtSA: a web application for calculating sequence specific protein solvent accessibilities in the unfolded ensemble. BMC Bioinform 2009;10:1–8. https://doi.org/10.1186/1471-2105-10-104.
[41] Peters GH, Olsen OH, Svendsen A, Wade RC. Theoretical Investigation of the Dynamics of the active Site Lid in *Rhizomucor miehei* Lipase. Biophys J 1996;71: 119–29.
[42] Santarossa G, Lafranconi PG, Alquati C, DeGioia L, Alberghina L, Fantucci P, et al. Mutations in the "lid" region affect chain length specificity and thermostability of a *Pseudomonas fragi* lipase. FEBS Lett 2005;579:2383–6. https://doi.org/10.1016/j.febslet.2005.03.037.
[43] Chen D, Oezguen N, Urvil P, Ferguson C, Dann SM, Savidge TC. Regulation of protein-ligand binding affinity by hydrogen bond pairing. Sci Adv 2016;2:1–16. https://doi.org/10.1126/sciadv.1501240 e1501240.
[44] Kumar A, Dhar K, Kanwar SS, Arora PK. Lipase catalysis in organic solvents: advantages and applications. Biol Proced Online 2016;18:1–11. https://doi.org/10.1186/s12575-016-0033-2.
[45] Inoue A, Horikoshi K. A Pseudomonas thrives in high concentrations of toluene. Nature 1989;338:264–6. https://doi.org/10.1038/338264a0.
[46] Meredith SC. Protein Denaturation and Aggregation. Cellular responses to Denatured and Aggregated Proteins. Ann NY Acad Sci 2005;1066:181–221. https://doi.org/10.1196/annals.1363.030.
[47] Pace CN, Treviño S, Prabhakaran E, Scholtz JM. Protein structure, stability and solubility in water and other solvents. Philos Trans R Soc Lond B Biol Sci 2004;359 (1448):1225–35. https://doi.org/10.1098/rstb.2004.1500.
[48] Sharma A, Dalai AK, Chaurasia SP. Thermodynamic study of hydrolysis and esterification reactions with immobilized lipase. Eur Int J Sci Technol 2015;4:128–36 ISSN: 2304-9693.
[49] Ghori MI, Iqbal MJ, Hameed A. Characterization of a novel lipase from Bacillus sp. isolated from tannery wastes. Braz J Microbiol 2011;42:22–9. https://doi.org/10.1590/S1517-83822011000100003.
[50] Åqvist J, Kazemi M, Isaksen GV, Brandsdal BO. Entropy and Enzyme Catalysis. Acc Chem Res 2017;50(2):199–207. https://doi.org/10.1021/acs.accounts.6b00321.
[51] Revell LE, Williamson BE. Why are some Reactions slower at higher Temperatures? J Chem Educ 2013;90(8):1024–7. https://doi.org/10.1021/ed400086w.
[52] Musa S, Latip W, Rahman RNZRA, Salleh AB, Ali MSM. Immobilization of an Antarctic Pseudomonas AMS8 Lipase for Low Temperature Ethyl Hexanoate Synthesis. Catalysts 2018;8(234):1–18. https://doi.org/10.3390/catal8060234.